BIOCHEMISTRY
including biophysical chemistry & molecular biology
Article

Biochemistry **2009,** *48,* 11655–11663 11655
DOI: 10.1021/bi901265z

The Heparin Binding Motif of Endostatin Mediates Its Interaction with Receptor Nucleolin†

Yan Fu,[‡,§,∥] Yang Chen,[‡,§,∥] Xu Luo,[‡,§,∥] Yun Liang,[‡,§,∥] Hubing Shi,[‡,§,∥] Lei Gao,[‡] Shunli Zhan,[‡] Daifu Zhou,[‡] and Yongzhang Luo*[,‡,§,∥]

[‡]*National Engineering Laboratory for Anti-tumor Protein Therapeutics,* [§]*Beijing Key Laboratory of Protein Therapeutics,* [∥]*Cancer Biology Laboratory, School of Life Sciences, and Tsinghua University, Beijing 100084, P. R. China*

Received July 24, 2009; Revised Manuscript Received October 24, 2009

ABSTRACT: Endostatin is a potent angiogenesis inhibitor with heparin-dependent activities. Nucleolin, a novel functional receptor of endostatin, mediates both the internalization to endothelial cells and the antiangiogenic activity of endostatin. To define the exact role of the heparin binding motif in mediating the interaction between endostatin and its receptor nucleolin, up to six arginine residues (R155, R158, R184, R270, R193, and R194) located in the heparin binding motif of endostatin were substituted by alanine to make double, quadruple, or hexad point mutations, respectively. Contributions of the heparin binding motif to both the interaction with nucleolin and the biological activities of endostatin were investigated from *in vitro* to *in vivo*. Here we show that Arg to Ala point mutagenesis of the heparin binding motif does not interrupt the folding of endostatin but significantly impairs the interaction between endostatin and nucleolin. Double and quadruple mutants showed significantly decreased internalization to endothelial cells and antitumor activities, while the hexad Arg to Ala mutant completely lost its interaction with nucleolin and biological functions. Taken together, the present study demonstrates that the arginine clusters in the heparin binding motif of endostatin significantly contribute to its interaction with receptor nucleolin and mediate the antiangiogenic and antitumor activities of endostatin.

Endostatin (ES),[1] a 20 kDa C-terminal proteolytic fragment of collagen XVIII, is a potent angiogenesis inhibitor and shows distinct binding to heparin (*1*). An extensive basic patch constituted by 11 clustered arginine residues was revealed by the crystal structure of mouse endostatin (*2*). Side chain modifications predicted the existence of the heparin binding motif of ES, which was composed of several clustered arginines but not the lysines (*3*). Using site-directed mutagenesis, Sasaki et al. further confirmed that a major site of Arg cluster (R155/R158/R184/R270) and a minor site of Arg cluster (R193/R194) of ES were essential for heparin or heparan sulfate binding (*4*). Moreover, the minor site containing the two clustered arginine residues (R193/R194) was proven to be critical for the inhibitory effect of ES on both FGF-2- and VEGF-A-induced angiogenesis thereafter (*5*).

Nucleolin (NL) was originally defined as a multifunctional nucleolar protein (*6*), which plays critical roles in nucleolar chromatin organization, pre-RNA packaging, rDNA transcription, and ribosome assembly during cell proliferation (*7*−*9*). Interestingly, NL was later reported to translocate from the nucleus to the cell surface in proliferating endothelial cells and serves as a marker for angiogenic vasculature (*10*). Moreover, certain angiogenesis factors including vascular endothelial growth factor (VEGF) and extracellular matrix (ECM) are involved in modulating the translocation process of NL (*11*).

Cell surface NL was further identified by our group as a novel functional ES receptor, which mediates the antiangiogenic and antitumor functions of ES (*12*). In this study, NL serves as a shuttle protein between the cytoplasm and the nuclei, thus mediating the internalization of ES into endothelial cells and the subsequent antiendothelial activity. Blocking cell surface nucleolin resulted in the loss of antiendothelial activity of ES. Moreover, ES binds to NL with a high affinity (K_D = 2.32 × 10^{-8} M), and they colocalize on the surface of endothelial cells on the angiogenic blood vessels in tumor tissues. Compared with other ubiquitous ES binding proteins in previous reports, the specific distribution of NL on the blood vessels in tumor tissues rather than normal tissues explains the specificity of ES function on the proliferating endothelial cells and its low toxicity in clinical trials (*12*, *13*). On the other hand, ES showed heparin-dependent antiendothelial activities in previous studies (*14*, *15*), suggesting that the heparin binding motif is involved in mediating the biological functions of ES. However, the critical amino acid residues involved in the interaction between ES and NL and the contribution of the heparin binding motif of ES to this interaction remain largely unelucidated.

Since Arg155, Arg184, Arg158, Arg270, Arg193, and Arg194 of ES were demonstrated to be the critical sites for heparin binding by Sasaki et al. (*5*, *16*), site-directed mutagenesis of Arg

†This work was supported in part by the General Programs of National Natural Science Foundation of China (No. 30670419 and No. 30771083), the National High Technology Research and Development Program of China (No. 2007AA02Z155), and the State Key Development Program for Basic Research of China (No. 2006CB910305).

*Address correspondence to this author. Tel: 86-10-6277-2897. Fax: 86-10-6279-4691. E-mail: yluo@tsinghua.edu.cn.

[1]Abbreviations: ES, endostatin; NL, nucleolin; All Ala, R155A/R158A/R184A/R270A/193A/R194A hexad mutant of endostatin; CD, circular dichroism; FL, Trp emission fluorescence; FACS, fluorescence activated cell sorting; SPR, surface plasmon resonance; HMECs, human microvascular endothelial cells.

Published on Web 10/30/2009

to Ala was performed to investigate whether or not these Arg residues are involved in the interaction between ES and its receptor NL. Five ES mutants were constructed, which include three mutants containing double mutation (R155A/R184A, R158A/R270A, and R193A/R194A), one containing quadruple mutation (R155A/R158A/R184A/R270A), and one containing hexad mutation (R155A/R158A/R184A/R270A/193A/R194A) (referred to as All Ala). The current study showed that double or quadruple Arg to Ala mutagenesis significantly impaired the interaction between ES and NL, as detected by coimmunoprecipitation and surface plasmon resonance (SPR) assays. Moreover, the binding and the internalizations of the double or quadruple ES mutants to endothelial cells were also dramatically attenuated, which caused a depletion of about 50% of the antiangiogenic and antitumor activities of ES. In addition, the All Ala mutant failed to interact with NL and showed undetectable biological activities. Collectively, the current study demonstrates that the heparin binding motif of ES mediates its interaction with receptor NL, which provides fundamental explanations to the heparin-dependent biological functions of ES.

MATERIALS AND METHODS

Antibodies, Proteins, Chemicals, and Cell Lines. Mouse anti-ES monoclonal antibody was purchased from Oncogene (USA). Other recombinant proteins and antibodies (ES, NL, rabbit anti-ES polyclonal antibody, and rabbit anti-NL polyclonal antibody) were generous gifts from Protgen Ltd. (Beijing, China). His-tagged recombinant human NL was expressed in a soluble form in *Pichia pastoris* (*12*). His-tagged ES and its mutants were expressed in *Escherichia coli* and refolded into native form thereafter, which followed the methods described by our previous studies (*12*, *17*). Chemicals including 6mer heparin were purchased from Sigma-Aldrich (Poole, U.K.) and Yili (Beijing, China). Human microvascular endothelial cell (HMEC) is an HDMEC cell line (catalog no. 2000, Sciencell) transfected with SV40 large T antigen, cultured with DMEM with 10% FBS according to previous reports (*11*, *12*, *18*). Lewis lung carcinoma (LLC) cells were purchased from the American Type Culture Collection (Manassas, VA).

Circular Dichroism (CD) Spectroscopy. Far-UV circular dichroism (CD) measurements were carried out on a Jasco-715 spectropolarimeter following the procedure described in our previous study (*17*) with modifications. Briefly, ES or ES mutant stocks were diluted in 5 mM Tris-HCl containing 0.9% NaCl, pH 7.4, to the final concentration of 10 μM. All measurements were performed at 37 °C.

Tryptophan Emission Fluorescence. Trp emission fluorescence (FL) spectra of ES and ES mutants were measured by a Hitachi F-4500 spectrophotometer equipped with a temperature-controlled liquid system as described by Zhou et al. (*17*) with modifications. Briefly, the concentrations of ES or ES mutants in 5 mM Tris-HCl containing 0.9% NaCl were 0.5 μM, and all measurements were carried out at 37 °C, pH 7.4.

Coimmunoprecipitation Assay in Vitro. ES or ES mutant (5 μg/mL) and NL (5 μg/mL) were coincubated in PBS (1 mL) with or without heparin (10 μM for heparin positive group) at 4 °C for 1 h. Then the rabbit anti-NL polyclonal antibody (1 μg/mL) and protein A−Sepharose beads (15 μL; Santa Cruz, CA) were added into the coimmunoprecipitation system and incubated for 3.5 h at 4 °C. The protein A−Sepharose beads were washed with TNE buffer (20 mM Tris, pH 7.4, with 0.5% NP40, 150 mM sodium chloride, 2 mM EDTA, 0.5 mM phenylmethanesulfonyl fluoride, and 1 × protease inhibitor mixture (Roche)) three times at 4 °C. Precipitated proteins were mixed with 2 × SDS loading buffer at 100 °C for 5 min. The samples were then applied to 12% SDS−PAGE and immunoblots with the rabbit anti-ES polyclonal antibody.

SPR Binding Assays. Surface plasmon resonance (SPR) measurements were performed according to the procedure described by Shi et al. (*12*) with modifications. Briefly, NL (100 μg/mL equivalent to 1250 nM) was immobilized on the surface of a CM5 sensor chip. ES/ES mutant solutions at concentrations of 5000, 2500, and 1250 nM were injected in a volume of 35 μL at the speed of 5 μL/min. After 7 min, the solutions containing ES/ES mutant were replaced with HEPES buffer, and the complexes were allowed to dissociate for 2 min. All experiments were performed with the BIAcoreX (GE) biosensor system, and the primary data were analyzed using the BIAevaluation 3.1 software (BIAcore AB) provided by the manufacturer.

Flow-Cytometry Analysis for Cell Surface Proteins. HMECs were harvested with 1 mM EDTA in phosphate-buffered saline (PBS) after 0.5 h incubation with ES. For NL blockage, the HMECs were preincubated with rabbit anti-NL polyclonal antibody on ice for 0.5 h before being treated by ES or All Ala. HEMCs were further incubated with 5 μg/mL primary monoclonal antibody against ES (anti-ES) in 100 μL of PBS containing 0.1% (w/v) bovine serum albumin (BSA) on ice for 0.5 h. An appropriately matched isotype at the same concentration as anti-ES served for the control group. Cells were washed twice with cold PBS containing 0.1% (w/v) BSA and stained with FITC-conjugated goat anti-mouse IgG (Santa Cruz, CA) in a 1:200 dilution on ice for 20 min. Cells were washed twice with cold PBS containing 0.1% (w/v) BSA and then analyzed with a FACS Calibur flow cytometry system (Becton Dickinson, San Jose, CA).

Internalization Assay. HMECs were seeded into 12-well plates with DMEM containing 10% fetal bovine serum and cultured for 24 h. After 8 h serum starvation (1% FBS) in DMEM, cells were incubated in DMEM medium, 2% FBS, and 5 ng/mL bFGF containing 10 μg/mL biotin-labeled wild-type ES or its mutants. HMECs in the heparin positive group were incubated with an additional 10 μM heparin during the serum deprivation and the internalization assay. At indicated time intervals, the treated cells were washed with PBS, fixed with 4% paraformaldehyde for 30 min, permeabilized with 0.2% Triton X-100, and blocked with 10% normal goat serum in PBS for 1 h. Then the cells were incubated with 1:400 TRITC-conjugated streptavidin (Pierce) for 30 min and 0.1 mg/mL DAPI for 1 min. The photographs were taken under the TRITC wavelength and the DAPI wavelength with an Olympus Fluoview laser scanning confocal imaging system, respectively.

Tumor Growth Assay. Lewis lung carcinoma (LLC) cells (2×10^6 per 100 μL) were inoculated in the subcutaneous space of C57BL/6 mice (6−8 weeks old). Saline, ES, or its mutants (1.5 mg/kg per day) were injected subcutaneously into the C57BL/6 mice at a site remote from the inoculated tumor after the tumor volume approached 0.1 cm^3. After seven daily injections, the mice were sacrificed, and the tumors were resected, photographed, weighed, and applied to immunohistochemistry.

The blood vessels in tumor tissues were labeled with anti-CD31, and the average number of blood vessels was counted from five random fields per section at 40× magnification. On the other hand, another group of sections was detected with DAPI,

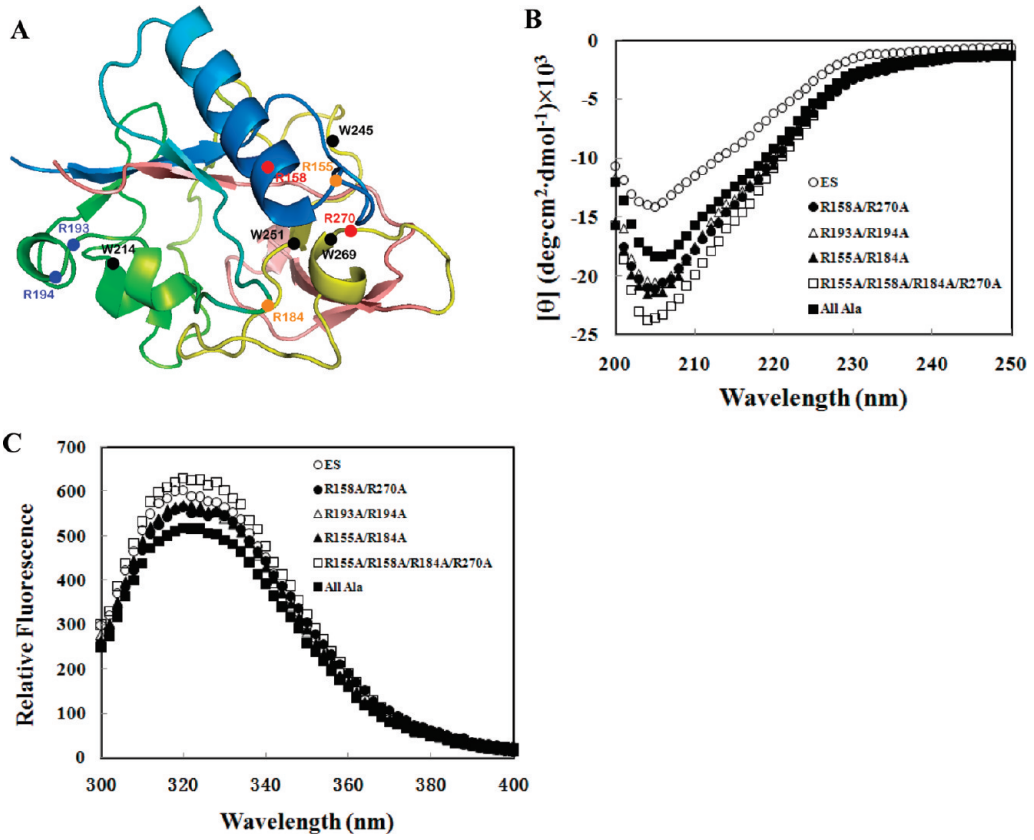

FIGURE 1: Spatial interpretation of the heparin binding motif of ES and the conformation analysis of ES and ES mutants. (A) Cartoon presentation of the ES structure. Positions of arginine residues of each double mutation in the current study were depicted in the same color on the ES molecule. R158 and R270 were labeled in red, R193 and R194 were in blue, and R155 and R184 were in orange. Four Trp residues (W214, W245, W251, and W269) were labeled in black. (B) The secondary structure of ES and ES mutants detected by circular dichroism spectra (CD). (C) The tertiary structure of ES and ES mutants detected by Trp fluorescence emission spectra (FL). All measurements were carried out in 5 mM Tris-HCl buffer containing 0.9% NaCl, pH 7.4, at 37 °C. The concentrations of ES and ES mutants were 10 and 0.5 μM for CD and FL, respectively.

murine anti-His-tag antibody (which was used to detect the His-tagged ES or ES mutants) followed by TRITC-conjugated goat anti-mouse IgG, and rabbit anti-NL polyclonal antibody followed by FITC-conjugated goat anti-rabbit IgG, respectively. Confocal fluorescence imaging was obtained on an Olympus Fluoview laser scanning confocal imaging system.

Statistical Methods. Statistical significance was assessed using Student's t test. P values were obtained by comparison between indicated groups. $P < 0.05$ was considered to be statistically significant. Data were presented as mean ± SD.

RESULTS

Contribution of the Heparin Binding Motif to the Conformation of Endostatin. Six arginine residues including Arg155, Arg158, Arg184, Arg193, Arg194, and Arg270 were reported to be critical for heparin binding in the ES molecule (*5*, *16*). To investigate the role of the heparin binding motif in mediating the interaction between ES and NL, these arginine residues were substituted by Ala either in double, quadruple, or hexad in the current study (Figure 1A). Circular dichroism (CD) and tryptophan emission fluorescence (FL) were used to detect the secondary and the tertiary structure of ES and its mutants under physiological temperature, respectively (*19*, *20*).

Based on the CD spectra, the amounts of the secondary structures (α-helix, β-sheet, and random coil) in all of the ES mutants are significantly more than that of the wild-type ES at 37 °C (Figure 1B). Double mutants R158A/R270A, R193A/R194A, and R155A/R184A have similar secondary structures (Figure 1B). Quadruple mutant R155A/R158A/R184A/R270 has more secondary structure than that of the double mutants. Surprisingly, the All Ala mutant (hexad mutant) has even less amount of secondary structure than that of the double mutants.

When excited at 288 nm, the wild-type ES showed the maximal Trp fluorescence emission wavelength (λ_{max}) at 318 nm, indicating a very compact folding of the tertiary structure (Figure 1C). There is no obvious change in the λ_{max} for all the mutants compared with the wild-type ES, which suggests a relatively stable core structure of ES upon mutating up to six arginine residues at physiological temperature. The fluorescence spectra of R158A/R270A, R193A/R194A, and R155A/R184A were superimposed, and the decreased fluorescence intensity suggests that their tertiary structures are a little more compact than that of the wild-type ES. In contrast, mutant R155A/R158A/R184A/R270A showed a looser structure than the wild-type ES, as evidenced by the increased fluorescence intensity around 318 nm (Figure 1C). Surprisingly, the All-Ala mutant exhibited a dramatic decrease in the fluorescence intensity around 318 nm, which suggests that its tertiary structure is more tightly packed than that of the wild-type ES and all of the other mutants (Figure 1C). These observations demonstrate that the Arg to Ala mutagenesis does not change the core structure of ES. However, the changes in the abundance of the secondary structure and the package of the tertiary structure suggest

substantial conformational change in certain local structures on ES molecule, which in turn may have a profound effect on their biological functions.

The Heparin Binding Motif Mediates the Interaction between Endostatin and Its Receptor Nucleolin in Vitro. Nucleolin (NL) was recently identified by our group as a functional ES receptor, which mediates the biological activities of ES (*12*). To investigate the contribution of the heparin binding motif to the interaction between ES and NL, coimmunoprecipitation assays of ES/ES mutants and NL were thus performed (Figure 2A). Mutants R158A/R270A, R193A/R194A, and R155A/R184A coimmunoprecipitated with NL, but the precipitating amounts were dramatically decreased when compared with that of the wild-type ES (Figure 2A). Hardly any detectable interaction between mutant R155A/R158A/R184A/R270A and NL was observed, and no interaction was detected between the All Ala mutant and NL (Figure 2A). Given the fact that the rabbit anti-ES polyclonal antibody recognizes ES and ES mutants with similar affinities (Supporting Information Figure S1), these results together demonstrate that the arginine residues tested in the current study are involved in the interaction between ES and its receptor NL. Site-directed mutagenesis on this heparin binding motif of ES impairs or completely disrupts such interactions.

In addition, preincubation of the wild-type or mutant ES with 10 μM 6mer heparin decreased their interactions with NL to a very low level (Figure 2A), which suggests that heparin competes with NL for the same binding sites of ES. Furthermore, we also compared the effects of 6mer and higher molecular weight heparin (mainly 8mer and 12mer) on interrupting the ES−NL interaction. Both types of heparin showed a concentration-dependent manner in blocking the interaction between ES and NL, although there was not much difference in the inhibitory potencies between these two types (Supporting Information Figure S2). Since heparin molecules are highly sulfated, to test if the blocking on the ES−NL interaction is heparin specific, sodium sulfate was thus employed. Not surprisingly, sodium sulfate did not block the interaction between ES and NL, even though there was a 50−100-fold molar excess of sulfate to the heparin used in this study (Supporting Information Figure S3). These observations together demonstrate that the blockage of heparin on the interaction between ES and NL is not due to nonspecific polyelectrolyte effects.

The interactions between ES/ES mutants and NL were quantified using surface plasmon resonance (SPR) binding assay, in which ES or ES mutants were allowed to first associate to and then dissociate from NL immobilized on the sensor chip. Different binding intensities of ES/ES mutants and NL were detected by the response units (RU) obtained from the same NL sensor ship and the same protocol. Five thousand nanomolar wild-type ES exhibited 420 RU of response, and the RU of mutants R158A/R270A, R193A/R194A, and R155A/R184A under the same concentration were 158, 149, and 224, respectively (Figure 2B). The significantly decreased RU values of the double mutants indicate that they lost up to 65% NL binding compared with the wild-type ES. Moreover, very weak response signals were detected with mutant R155A/R158A/R184A/R270A (18 RU) and All Ala (1.3 RU) (Figure 2B), which demonstrates very tiny interactions between these two mutants and NL. These observations are highly consistent with the coimmunoprecipitation assay. In addition, kinetic parameters were obtained from different concentration gradients of ES and ES double mutants.

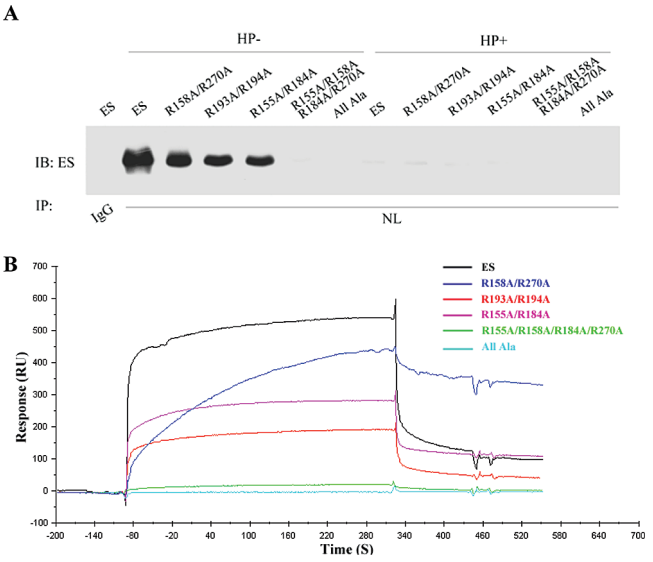

FIGURE 2: Interactions between ES/ES mutants and NL. (A) Coimmunoprecipitation of ES/ES mutants and NL in the absence or presence of 10 μM heparin. Indicated concentrations of ES or ES mutants, NL, and heparin (added in the HP+ group) were coincubated for 2 h. The ES−NL complex was immunoprecipitated by anti-NL antibody and was applied to IB using rabbit anti-ES polyclonal antibody. (B) SPR binding assay between ES/ES mutants and NL. NL (100 μg/mL equivalent to 1250 nM) was immobilized on the surface of a CM5 sensor chip. Response units (RU) of ES/ES mutant at the concentration of 5000 nM, k_a, and K_D derived from different concentration gradients were obtained using the BIAevaluation 3.1 software.

The k_a values for R158A/R270A, R193A/R194A, and R155A/R184A were 5.55 1/M·s, 351 1/M·s, and 57.1 1/M·s, respectively, which were much lower than that of the wild-type ES (930 1/M·s). These observations indicate that all of the double mutants bind to NL at significantly decreased rates compared with the wild-type ES, and R158 and R270 are extremely critical for the binding kinetics between ES and NL. The K_D values of ES, R158A/R270A, R193A/R194A, and R155A/R184A were 7.01×10^{-7} M, 8×10^{-5} M, 1.95×10^{-6} M, and 5.06×10^{-7} M, respectively, which shows that the binding affinities of these mutants with NL are lower than that of the wild-type ES. It should be pointed out that the K_D in this study was obtained on the immobilized NL, which was different from our previous data (2.32×10^{-8} M) determined on immobilized ES (*12*).

Since up to six Arg mutations in the heparin binding motif did not change the core structure of ES (Figure 1B,C) but significantly attenuated its interaction with receptor NL (Figure 2), it is quite plausible that the core structure contributes more to the overall conformation and stability of ES, while the surface amino acid residues such as the arginine clusters contribute more to the binding to nucleolin.

The Heparin Binding Motif of Endostatin Is Involved in Its Binding to Endothelial Cells and the Subsequent Internalization. Since ES was reported to bind to NL on the endothelial cell surface (*12*) and Arg mutations disrupted the interaction between ES and NL (Figure 2), we were thus prompted to test if the binding affinity of ES to endothelial cells was affected by these mutations. In this regard, flow cytometry assays were performed on human microvascular endothelial cells (HMECs) with ES and its mutants, respectively. Mouse anti-ES monoclonal antibody, which recognizes ES and ES mutants with similar affinities (Supporting Information Figure S1), was

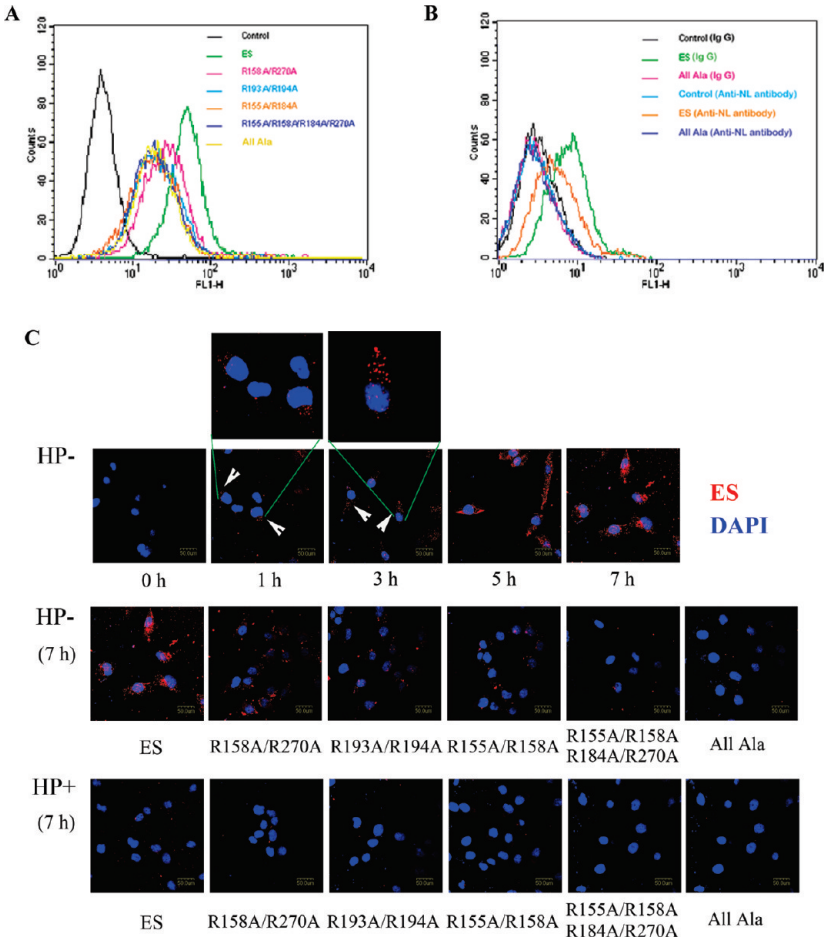

FIGURE 3: The binding capacity and internalization of ES or ES mutants to HMECs. (A) The binding of ES or ES mutants to the HMECs surface was measured by flow cytometry. Cell surface ES or ES mutants were stained with saturating amounts of monoclonal antibody recognizing ES and evaluated by flow cytometric analysis. (B) Anti-NL antibody blocked the binding of ES to the surface of HMECs. HMECs were preincubated with rabbit anti-NL polyclonal antibody before being treated with ES or All Ala mutant. ES or All Ala bound to the HMECs was detected by mouse anti-ES monoclonal antibody. IgG served as negative control for the blockade of cell surface NL. (C) Internalization of ES or ES mutants by HMECs in the absence or presence of 10 μM heparin. The upper shows the internalization of the wild-type ES in the absence of heparin at indicated time intervals (0, 1, 3, 5, and 7 h), among which critical cells were shown in enlarged images. Internalizations of ES or ES mutants (red) to HMECs in the absence or presence of 10 μM heparin at 7 h were shown in the middle and lower panels, respectively. Blue color stands for DAPI in all images.

employed for the detection of cell surface ES and its mutants. Figure 3A showed that the binding capacities of ES mutants to the surface of HMECs were about 50% of that of the wild-type ES. Moreover, anti-NL antibody significantly blocked the binding of the wild-type ES to the surface of HMECs (Figure 3B), which demonstrates that NL is a very important ES binding protein on the endothelial cell surface. In addition, only very small portions of HMECs were detected to bind the wild-type ES or its mutants on the cell surface in the presence of heparin, which suggests that the heparin binding motif of ES is involved in the binding of ES to HMECs, and heparin can interrupt such binding efficiently (data not shown).

Since the Arg to Ala site-directed mutagenesis significantly impaired the binding capacities of ES to HMECs (Figure 3A) and ES was reported to be internalized upon binding to HMECs (*12*), it is reasonable to assume that the amount of internalized ES mutants should be much less than that of the wild-type ES. Time course internalization assays of ES and ES mutants were performed in the absence or presence of heparin. In the absence of heparin, the wild-type ES (red) was detected in the cytosol of HMECs after 1 h treatment, and more ES accumulated in HMECs after 3 h with a small amount appearing in the nuclei (Figure 3C, upper panel and enlarged images). At 5 and 7 h, a distinct amount of ES was detected both in the cytosol and in nuclei of HMECs (Figure 3C, upper panel). The internalization behaviors of the ES mutants in the absence of heparin were detected in the same manner, and representative fields at 7 h were shown in the middle panel of Figure 3C. The internalizations of ES mutants by HMECs at 7 h were significantly decreased compared with that of the wild-type ES, with the All Ala mutant showing the least amount of internalization (Figure 3C, middle panel). On the other hand, in the presence of heparin, even at 7 h, little ES, including the wild type or mutants, was internalized to HMECs (Figure 3C, lower panel). These observations strongly suggest that the heparin binding motif is involved in both the binding and the subsequent internalization of ES to HMECs.

Contribution of the Heparin Binding Motif to the Biological Functions of Endostatin. To further investigate the biological significance of the ES−NL interaction, the antiendothelial activity of ES and its mutants was compared using HMEC migration and wound healing assays in the absence or presence of heparin. The wild-type ES inhibited over 50% of HMECs migration in the absence of heparin, while only about 20% inhibition was observed in the groups treated with

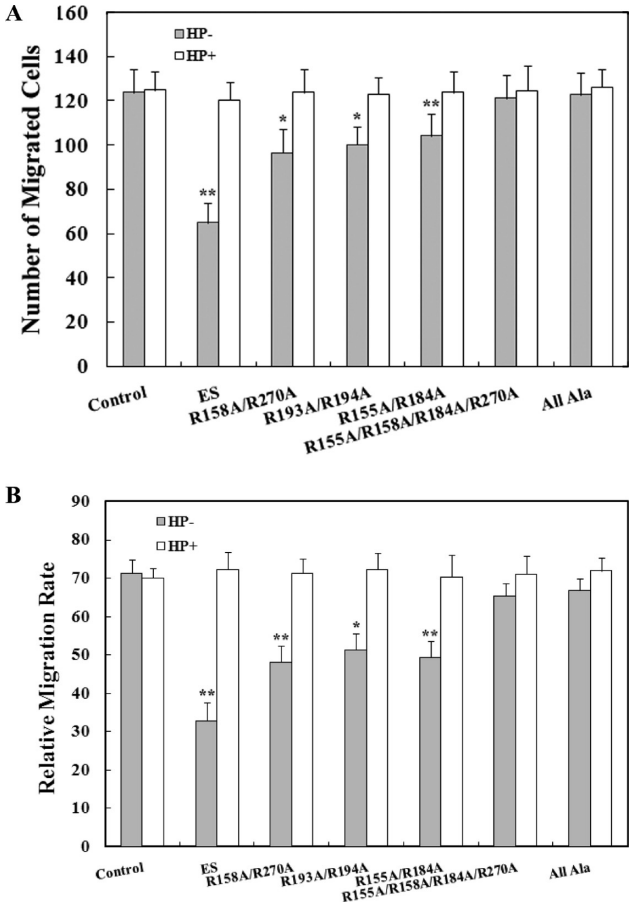

FIGURE 4: Quantified antiendothelial activity of ES and ES mutants in the absence or presence of 10 μM heparin. (A) Inhibition of ES and ES mutants on the HMEC migration tested by Transwell assay. (B) Inhibition of ES and ES mutants on the HMEC wound healing assay. The error bars represent mean values ± SD. *, $p < 0.05$; **, $p < 0.01$ vs control group. All experiments were repeated twice, and each sample was assayed at least in triplicate.

R158A/R270A, R193A/R194A, or R155A/R184A. In addition, mutants R155A/R158A/R184A/R270A and All Ala showed little if any inhibitory effect on the HMECs migration (Figure 4A and Supporting Information Figure S4A, upper panel). In the presence of 10 μM heparin, almost no inhibition on the HMECs migration was observed in the wild-type ES or ES mutant treated groups (Figure 4A and Supporting Information Figure S4A, lower panel). Similar results were obtained in the HMECs wound healing assays (Figure 4B and Supporting Information Figure S4B). Since NL is a major functional ES receptor (*12*), the potent blockage of heparin on the ES−NL interaction provides reasonable explanation to the heparin-dependent antiendothelial activity of ES. Moreover, the significant attenuation in the antiendothelial activity of ES caused by the Arg mutation indicates that these Arg residues are critical for the interaction between ES and NL.

Since mutations on the heparin binding motif of ES significantly impaired the interaction between ES and NL (Figure 2), we further examined the effect of this attenuated interaction on the antitumor and antiangiogenic activities of ES on the Lewis lung carcinoma (LLC) mouse model. The image of representative tumors and the average tumor weight of each group were shown in panels A and B of Figure 5, respectively. The tumor inhibition of the wild-type ES treated group was 64%, while those of mutants R158A/R270A, R193A/R194A, and R155A/R184A were 45%, 43%, and 31%, respectively. The tumor inhibition of mutant R155A/R158A/R184A/R270A was only 10%, and the All Ala mutant showed almost no antitumor activity (Figure 5A, B). This result is highly reproducible as shown in Supporting Information Figure S5. These *in vivo* studies show that the arginine clusters in the heparin binding motif indeed play important roles in the antitumor activity of ES. Then we further detected the blood vessel density in tumor tissues by CD31 staining. The upper panel of Figure 5C shows representative images of tumor blood vessels from each group. The lower panel of Figure 5C shows the quantified blood vessel density in each treatment group, which explained the antitumor activity shown in Figure 5A,B.

We also examined the colocalization of ES or ES mutants (red) with its receptor NL (green) in tumor tissues by immunohistochemistry (Figure 5D). In the wild-type ES, mutant R158A/R270A, mutant R193A/R194A, and mutant R155A/R184A treated groups, ES or ES mutants (red) colocalized with its receptor NL (green) in different amounts, which explained the variation in their antitumor and antiangiogenic activities shown in Figure 5A−C. Although NL was found in the tumor tissues from R155A/R158A/R184A/R270A and All Ala treated groups, neither of these ES mutants was detected (Figure 5D). Therefore, it is not surprising that R155A/R158A/R184A/R270A and All Ala have little antitumor and antiangiogenic activities.

In sum, site-directed mutagenesis on the heparin binding motif of ES distinctly interrupts the interaction between ES and NL, which in turn dramatically attenuates the biological functions of ES.

DISCUSSION

In the current study, double mutants of R158A/R270A, R193A/R194A, and R155A/R184A showed dramatically decreased antiendothelial, antiangiogenic, and antitumor activities compared with the wild-type ES. Even less bioactivity of ES was observed with quadruple mutant R155A/R158A/R184A/R270A, while the All Ala mutant exhibited little if any activity in both *in vitro* and *in vivo* experiments (Figures 4 and 5 and Supporting Information Figures S4 and S5). These are consistent with the previous report that Arg to Ala point mutation impaired the antiangiogenic activity of ES on CAM assays (*5*, *16*, *21*). The current study shows that upon Arg to Ala mutation in the heparin binding motif, ES maintains substantial native structure at physiological temperature (Figure 1B,C), which indicates that the loss of activity in ES mutants does not result from incorrect folding. Moreover, except W269 locates adjacently to R270 in the spatial conformation, the other three Trp residues (W214, W245, W251) locate a little bit further away from the Arg residues tested in the current study (Figure 1A). Although the core structure of ES appears not changed by the Arg to Ala mutagenesis, it is quite possible that the changes in the local secondary structures around the heparin binding motif may affect its binding with NL. Importantly, the present study demonstrates that the interaction with NL, the binding to HMECs, and the internalization by HMECs of ES are severely decreased upon Arg to Ala site-directed mutagenesis (Figures 2 and 3), which provides the key reason for the low bioactivities of ES mutants. These observations demonstrate that the heparin binding motif of ES mediates its interaction with receptor NL and verified the biological significance of such interaction.

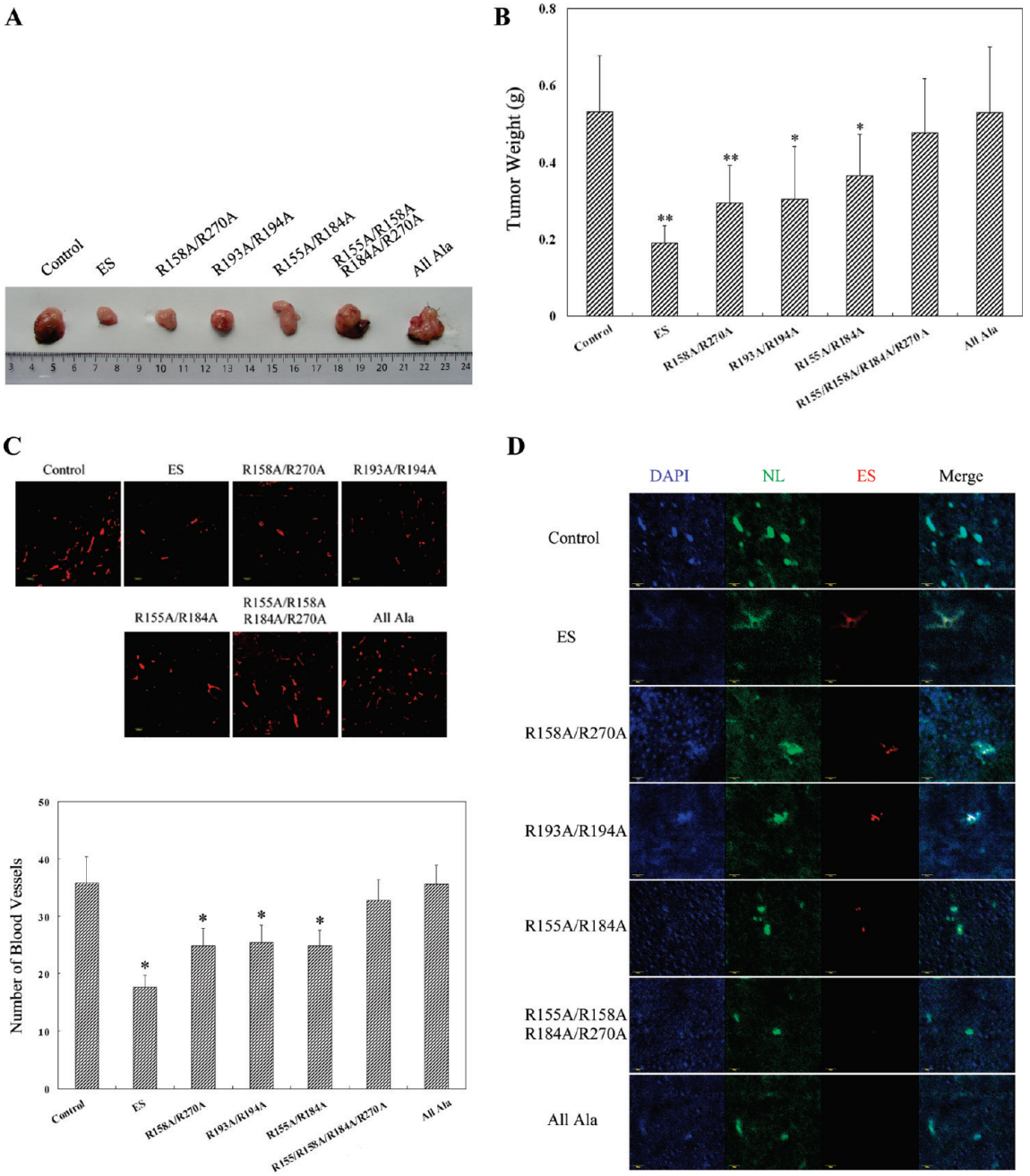

FIGURE 5: Antitumor activities of ES and ES mutants on Lewis lung carcinoma tested on the mouse model. (A) Photograph of a representative tumor in each group treated with ES, ES mutants, or saline as control. (B) Quantified tumor weight of each group treated with ES, ES mutants, or saline ($n = 6$) (*, $p < 0.05$; **, $p < 0.01$ vs control group). (C) Representative fields of the blood vessels in each group were stained with anti-CD31 (upper panel). Scale bar represents 100 μm. Quantified blood vessel density in tumor tissues counted from the representative fields of each treatment group (lower panel; *, $p < 0.01$). (D) Colocalization of ES or ES mutants with NL *in vivo* detected by immunohistochemical analysis. ES (red) was detected by murine anti-His-tag antibody followed by TRITC-conjugated goat anti-mouse IgG, and NL (green) was detected by rabbit anti-NL polyclonal antibody followed by FITC-conjugated goat anti-rabbit IgG, respectively. DAPI (blue) indicates cells in the fields. Scale bar represents 20 μm.

In this study, mutagenesis on Arg158/Arg270, Arg193/Arg194, and Arg155/Arg184 was verified to have equivalent influence on disrupting the biological functions of ES, while mutagenesis of Arg155/Arg158/Arg184/Arg270 showed an additive attenuation effect of mutant Arg158/Arg270 and mutant Arg155/Arg184 (Figures 4 and 5 and Supporting Information Figures S4 and S5). Structural analysis shows that Arg155, Arg158, Arg184, and Arg270 locate adjacently with each other, while Arg193 and Arg194 are relatively far away from these arginine residues (Figure 1A). It is hereby suggested that the primary NL binding site of ES is centered around Arg158 and Arg270, and the secondary binding site consists of Arg193 and Arg194. The positions of these two major NL binding sites of ES are consistent with the previously reported heparin binding sites (*4*). Moreover, the complete loss of both NL binding and biological activity in the All Ala mutant but not other mutants strongly indicates that NL simultaneously occupies these six arginine residues in the heparin binding motif of ES. This explains the relatively more critical role of Arg193 and Arg194 in the ES−NL interaction (Figure 2B), because if NL binds to ES through the bipartite binding interface, Arg193 and Arg194 probably serve as a nonreplaceable binding site compared with

either pair of the other four Arg residues. Thus we provide the first direct evidence for the exact amino acid residues mediating the interaction between ES and its receptor NL.

In addition, we show here that heparin oligosaccharides significantly block the antiendothelial activity of ES (Figure 4 and Supporting Information Figure S4), which is consistent with the previous report (*22*). This heparin effect is not due to nonspecific polyelectrolyte effects (Supporting Information Figure S3). Although 6mer and 8−12mer heparins were reported to bind to ES with different efficiencies (*22*), they show equivalent blockage effects on the interaction between ES/ES mutants and NL in the current study (Supporting Information Figure S2). The potential competition of heparin with NL in its binding with ES provides a molecular explanation to the open question of why the antiangiogenic activity of ES is heparin/heparan sulfate dependent (*14*, *15*) and also suggests that the clinical applications of ES should avoid heparin-like compounds.

Besides NL, a number of cell surface proteins including integrins, tropomyosin, glypicans, and MMP2 were reported to interact with ES (*23*−*26*). For example, $\alpha 5\beta 1$ integrins were proposed to act as ES receptors, and a potential integrin-binging sequence within ES was indicated by the antiendothelial activity of an ES-derived synthetic arginine-rich peptide (*23*, *27*). On the other hand, Reis et al. demonstrated that ES competes with basic fibroblast growth factor (bFGF) for the binding to heparan-like glycosaminoglycans and proposed the potential binding of ES with proteoglycan receptors *in vivo* (*28*). Cell surface proteoglycans glypican-1 and -4 were identified as low-affinity ES receptors, and the heparan sulfate glycosaminoglycans of glypicans were proven to be critical for such binding (*25*). Although we only focus on NL in the current study, we cannot exclude the possibility that ES binds to other proteins cooperatively or these proteins form ES coreceptors. The detailed molecular interaction between the heparin binding motif of ES and NL will be available after the cocrystal structure of ES and NL is resolved, which is being investigated. Unraveling the structural basis of the interaction between ES and NL will provide clues for the mechanistic elucidation of ES function and also shed light on the potential drug design for antitumor therapeutics.

ACKNOWLEDGMENT

We gratefully appreciate Lijun Chao and Yun Zhu at Tsinghua University for technical assistance in the SRP and FACS assays and Di Miao for technical assistance in the MALDI-TOF MS experiment. We also appreciate all of the members of the Luo Laboratory for constructive suggestions and insightful discussions throughout this work, Bipo Sun for laboratory routine management, and Protgen Ltd. for generous gifts of the protein and antibody samples.

SUPPORTING INFORMATION AVAILABLE

Figures showing the recognition of ES and ES mutants by the anti-ES monoclonal or polyclonal antibodies, the concentration-dependent heparin effect on ES−NL interaction, the anion effect of sodium sulfate on ES−NL interaction, and the representative images of the antiendothelial and antitumor activities of ES and ES mutants; methods of the purification of 8−12mer of heparin and the detection of ES−NL interaction by ELISA in the presence of different concentrations of heparin or sodium sulfate. This material is available free of charge via the Internet at http://pubs.acs.org.

REFERENCES

1. O'Reilly, M. S., Boehm, T., Shing, Y., Fukai, N., Vasios, G., Lane, W. S., Flynn, E., Birkhead, J. R., Olsen, B. R., and Folkman, J. (1997) Endostatin: An endogenous inhibitor of angiogenesis and tumor growth. *Cell 88*, 277–285.
2. Hohenester, E., Sasaki, T., Olsen, B. R., and Timpl, R. (1998) Crystal structure of the angiogenesis inhibitor endostatin at 1.5 angstrom resolution. *EMBO J. 17*, 1656–1664.
3. Sasaki, T., Fukai, N., Mann, K., Gohring, W., Olsen, B. R., and Timpl, R. (1998) Structure, function and tissue forms of the C-terminal globular domain of collagen XVIII containing the angiogenesis inhibitor endostatin. *EMBO J. 17*, 4249–4256.
4. Sasaki, T., Larsson, H., Kreuger, J., Salmivirta, M., Claesson-Welsh, L., Lindahl, U., Hohenester, E., and Timpl, R. (1999) Structural basis and potential role of heparin/heparan sulfate binding to the angiogenesis inhibitor endostatin. *EMBO J. 18*, 6240–6248.
5. Olsson, A. K., Johansson, I., Akerud, H., Einarsson, B., Christofferson, R., Sasaki, T., Timpl, R., and Claesson-Welsh, L. (2004) The minimal active domain of endostatin is a heparin-binding motif that mediates inhibition of tumor vascularization. *Cancer Res. 64*, 9012–9017.
6. Ginisty, H., Sicard, H., Roger, B., and Bouvet, P. (1999) Structure and functions of nucleolin. *J. Cell Sci. 112* (Part 6), 761–772.
7. Ginisty, H., Amalric, F., and Bouvet, P. (1998) Nucleolin functions in the first step of ribosomal RNA processing. *EMBO J. 17*, 1476–1486.
8. Erard, M. S., Belenguer, P., Caizergues-Ferrer, M., Pantaloni, A., and Amalric, F. (1988) A major nucleolar protein, nucleolin, induces chromatin decondensation by binding to histone H1. *Eur. J. Biochem. 175*, 525–530.
9. Kharrat, A., Derancourt, J., Doree, M., Amalric, F., and Erard, M. (1991) Synergistic effect of histone H1 and nucleolin on chromatin condensation in mitosis: Role of a phosphorylated heteromer. *Biochemistry 30*, 10329–10336.
10. Christian, S., Pilch, J., Akerman, M. E., Porkka, K., Laakkonen, P., and Ruoslahti, E. (2003) Nucleolin expressed at the cell surface is a marker of endothelial cells in angiogenic blood vessels. *J. Cell Biol. 163*, 871–878.
11. Huang, Y. J., Shi, H. B., Zhou, H., Song, X. M., Yuan, S. P., and Luo, Y. Z. (2006) The angiogenic function of nucleolin is mediated by vascular endothelial growth factor and nonmuscle myosin. *Blood 107*, 3564–3571.
12. Shi, H. B., Huang, Y. J., Zhou, H., Song, X. M., Yuan, S. P., Fu, Y., and Luo, Y. Z. (2007) Nucleolin is a receptor that mediates antiangiogenic and antitumor activity of endostatin. *Blood 110*, 2899–2906.
13. Eder, J. P., Supko, J. G., Clark, J. W., Puchalski, T. A., Garcia-Carbonero, R., Ryan, D. P., Shulman, L. N., Proper, J., Kirvan, M., Rattner, B., Connors, S., Keogan, M. T., Janicek, M. J., Fogler, W. E., Schnipper, L., Kinchla, N., Sidor, C., Phillips, E., Folkman, J., and Kufe, D. W. (2002) Phase I clinical trial of recombinant human endostatin administered as a short intravenous infusion repeated daily. *J. Clin. Oncol. 20*, 3772–3784.
14. Gaetzner, S., Deckers, M. M. L., Stahl, S., Lowik, C., Olsen, B. R., and Felbor, U. (2005) Endostatin's heparan sulfate-binding site is essential for inhibition of angiogenesis and enhances in situ binding to capillary-like structures in bone explants. *Matrix Biol. 23*, 557–561.
15. Folkman, J. (2007) Endostatin finds a new partner: Nucleolin. *Blood 110*, 2786–2787.
16. Sasaki, T., Larsson, H., Kreuger, J., Salmivirta, M., Claesson-Welsh, L., Lindahl, U., Hohenester, E., and Timpl, R. (1999) Structural basis and potential role of heparin/heparan sulfate binding to the angiogenesis inhibitor endostatin. *EMBO J. 18*, 6240–6248.
17. Zhou, H., Wang, W., and Luo, Y. Z. (2005) Contributions of disulfide bonds in a nested pattern to the structure, stability, and biological functions of endostatin. *J. Biol. Chem. 280*, 11303–11312.
18. Ades, E. W., Candal, F. J., Swerlick, R. A., George, V. G., Summers, S., Bosse, D. C., and Lawley, T. J. (1992) HMEC-1: Establishment of an immortalized human microvascular endothelial cell line. *J. Invest. Dermatol. 99*, 683–690.
19. Li, B., Wu, X. Y., Zhou, H., Chen, Q. J., and Luo, Y. Z. (2004) Acid-induced unfolding mechanism of recombinant human endostatin. *Biochemistry 43*, 2550–2557.
20. Fu, Y., Wu, X. Y., Han, Q., Liang, Y., He, Y. B., and Luo, Y. Z. (2008) Sulfate stabilizes the folding intermediate more than the native structure of endostatin. *Arch. Biochem. Biophys. 471*, 232–239.
21. Dixelius, J., Larsson, H., Sasaki, T., Holmqvist, K., Lu, L., Engstrom, A., Timpl, R., Welsh, M., and Claesson-Welsh, L. (2000) Endostatin-induced tyrosine kinase signaling through the Shb adaptor protein regulates endothelial cell apoptosis. *Blood 95*, 3403–3411.

22. Kreuger, J., Matsumoto, T., Vanwildemeersch, M., Sasaki, T., Timpl, R., Claesson-Welsh, L., Spillmann, D., and Lindahl, U. (2002) Role of heparan sulfate domain organization in endostatin inhibition of endothelial cell function. *EMBO J. 21*, 6303–6311.
23. Rehn, M., Veikkola, T., Kukk-Valdre, E., Nakamura, H., Ilmonen, M., Lombardo, C. R., Pihlajaniemi, T., Alitalo, K., and Vuori, K. (2001) Interaction of endostatin with integrins implicated in angiogenesis. *Proc. Natl. Acad. Sci. U.S.A. 98*, 1024–1029.
24. MacDonald, N. J., Shivers, W. Y., Narum, D. L., Plum, S. M., Wingard, J. N., Fuhrmann, S. R., Liang, H., Holland-Linn, J., Chen, D. H. T., and Sim, B. K. L. (2001) Endostatin binds tropomyosin—A potential modulator of the antitumor activity of endostatin. *J. Biol. Chem. 276*, 25190–25196.
25. Karumanchi, S. A., Jha, V., Ramchandran, R., Karihaloo, A., Tsiokas, L., Chan, B., Dhanabal, M., Hanai, J. I., Venkataraman, G., Shriver, Z., Keiser, N., Kalluri, R., Zeng, H., Mukhopadhyay, D., Chen, R. L., Lander, A. D., Hagihara, K., Yamaguchi, Y., Sasisekharan, R., Cantley, L., and Sukhatme, V. P. (2001) Cell surface glypicans are low-affinity endostatin receptors. *Mol. Cell 7*, 811–822.
26. Kim, Y. M., Jang, J. W., Lee, O. H., Yeon, J., Choi, E. Y., Kim, K. W., Lee, S. T., and Kwon, Y. G. (2000) Endostatin inhibits endothelial and tumor cellular invasion by blocking the activation and catalytic activity of matrix metalloproteinase 2. *Cancer Res. 60*, 5410–5413.
27. Wickstrom, S. A., Alitalo, K., and Keski-Oja, J. (2004) An endostatin-derived peptide interacts with integrins and regulates actin cytoskeleton and migration of endothelial cells. *J. Biol. Chem. 279*, 20178–20185.
28. Reis, R. C. M., Schuppan, D., Barreto, A. C., Bauer, M., Bork, J. P., Hassler, G., and Coelho-Sampaio, T. (2005) Endostatin competes with bFGF for binding to heparin-like glycosaminoglycans. *Biochem. Biophys. Res. Commun. 333*, 976–983.